Electronic Research Archive

http://www.aimspress.com/journal/era

ERA, 33(1): 381–408.
DOI: 10.3934/era.2025019
Received: 18 November 2024
Revised: 24 December 2024
Accepted: 06 January 2025
Published: 23 January 2025

Research article

Mechanism- and data-driven algorithms of electrical energy consumption accounting and prediction for medium and heavy plate rolling

Qiang Guo[1], Zimeng Zhou[2], Jie Li[1] and Fengwei Jing[1,*]

[1] National Engineering Research Center for Advanced Rolling and Intelligent Manufacturing, University of Science and Technology Beijing, Beijing 100083, China

[2] School of Automation and Electrical Engineering, University of Science and Technology Beijing, Beijing 100083, China

* **Correspondence:** Email: jingfengwei@nercar.ustb.edu.cn.

Abstract: Energy consumption accounting and prediction in the medium and thick plate rolling process are crucial for controlling costs, improving production efficiency, optimizing equipment management, and enhancing the market competitiveness of enterprises. Starting from the perspective of integrating process mechanism and industrial big data, we overcame the difficulties brought by complex and highly nonlinear coupling of process variables, proposed a rolling power consumption accounting algorithm based on time slicing method, and gave a calculation method for the additional power consumption of the main motor for rough rolling and finishing rolling (auxiliary system power consumption, power loss, main motor power consumption deviation); with the help of SIMS model, forward recursion, and reverse recursion pass rolling force estimation strategies are proposed, and the rated power consumption of the main motor was predicted. Furthermore, a random forest regression model of additional power consumption based on data was established, and then a prediction algorithm for the comprehensive power consumption of billet rolling was given. Experiments showed the effectiveness of the proposed method.

Keywords: medium-thick plate rolling; electrical power consumption calculation; electrical power consumption; time-slice method; SIMS model

1. Introduction

As a key material for infrastructure and heavy machinery manufacturing, medium and thick plates provide the necessary strength and stability and are an important pillar of modern industry and economic development [1, 2]. In the context of the "new normal" of the economy, energy, resource, and environmental constraints have gradually become the major factors restricting economic development.

With the increasing global attention to energy efficiency and carbon emissions, it is particularly important to accurately calculate and predict the power consumption of medium and thick plates during the rolling process. This will not only help improve production efficiency and reduce operating costs, but also support enterprises in implementing energy-saving measures and optimizing production processes to promote sustainable development. Furthermore, accurate prediction of electricity consumption provides data support for economic decision-making and environmental management of enterprises, promotes the rational allocation and utilization of resources, and helps achieve carbon peak and carbon neutrality goals. Therefore, the study of electricity consumption accounting and prediction in the thick plate rolling process has important academic value and broad application prospects [3, 4].

On the energy consumption calculation, some notable achievements have been made. G. P. Perunov et al. developed a method to determine the specific power consumption of reversible rolling, accounting for tension force, based on A. I. Tselikov's power-force parameters for thin sheet cold rolling and established methods for calculating power consumption in drum coilers and uncoilers [5]. M. Tan et al. proposed an economic load scheduling model for hot rolling under time-of-use electricity prices, minimizing electricity costs while factoring in penalties for slab transitions. They used a multi-objective scheduling algorithm (NSGA-II) and TOPSIS to recommend the optimal solution [6]. L. Giorleo et al. examined energy and force requirements during ring rolling, simulating preforms with varying initial heights to study their impact on final forming feasibility, energy, and force requirements [7]. J. Paralikas et al. introduced an energy-saving index for cold roll forming, developing a model to estimate energy consumption and productivity, and calculating the impact of key process parameters on the energy-saving index in U-section profiles [8]. V. Chubenko et al. used DEFORM-3D software to simulate the hot rolling process, optimizing energy consumption by analyzing force, stress, and displacement in the deformation zone [9]. J. Qiu et al. proposed an energy-saving delay strategy for heating furnaces, using simulation software to optimize delay temperature and slab energy consumption. Their approach significantly improved energy savings compared to traditional methods, with benefits increasing as delay time extended [10].

On the energy consumption prediction, there have been many valuable studies. To optimize operating variables, improve rolling quality, and reduce unit power consumption, X. Chen et al. used a data-driven approach with a neural network algorithm to create a prediction model linking performance and set values, and performed multi-objective optimization with equipment constraints [11]. Y. Zhong et al. proposed an energy consumption prediction model (ECPMM) for horizontal rough rolling, based on roller adaptive wear strategy, and introduced a two-directional adaptive differential evolution algorithm (TDADE) [12]. Y. K. Kim et al. developed a multi-level stacked regression model to predict the total power consumption of a hot rolling mill, using preprocessed operational data and derived variables related to power consumption [13]. X. Xiong et al. proposed a random forest prediction model based on principal component dimension reduction and artificial bee colony dynamic search fusion, predicting power consumption in the hot strip rolling finishing section [14]. S. Behzadipour et al. introduced a neural network-based power estimation model for shape rolling, incorporating a "shape factor" to quantify shape changes during rolling [15]. G. A. Orcajo et al. developed a method to replicate operating conditions in a hot rolling mill and predict changes in electrical variables, considering different steel grades and their impact on power demand and quality parameters [16].

There are many difficulties in calculating and predicting power consumption during the rolling process, mainly due to the complexity of the process. The rolling process of medium and thick plates

covers rough rolling, finishing rolling, cooling, straightening, and other links and involves multiple auxiliary systems and equipment such as transmission, lubrication, and dust removal. Furthermore, the rolling process is accompanied by various dynamic change factors such as material deformation, heat conduction, and friction, and the rolling speed, temperature, pressure, and other variables are highly coupled, which increases the complexity of power consumption calculation and prediction, making it difficult to achieve accurate prediction through simple models. In addition, the highly nonlinear relationship between power consumption and process variables and the uncertainty in the production process also bring difficulties to calculation and prediction. Uncertain factors such as temperature fluctuations, equipment wear, and changes in material properties during the rolling process often affect power consumption, increase the complexity of the model, and make it difficult for traditional models to accurately capture these relationships.

To overcome these difficulties and differ from approaches that typically use overall accounting and focus solely on either process mechanisms or data-driven techniques, we begin from the perspective of integrating metallurgical mechanism and industrial big data, and closely combine the rolling process characteristics of medium and thick plates to propose a systematic solution. By introducing the concept of time slicing and incorporating the idea of "divide and conquer", differentiated accounting methods are adopted for different links; forward recursion and reverse recursion pass rolling force estimation strategies are proposed, and the rated power consumption of the major motors for rough rolling and finishing rolling is calculated in combination with the rolling force model. Furthermore, to cope with the complexity and uncertainty in the production process, additional power consumption (auxiliary system power consumption, power loss, main motor power consumption deviation) is predicted using a data-driven method. This comprehensive strategy not only improves the accuracy of power consumption accounting and prediction, but also provides strong support for optimizing the rolling process.

The major contributions of this paper can be summarized as follows:

1) Power consumption accounting: we introduce a time-slice based rolling power consumption calculation algorithm. The algorithm adopts a modular approach, breaking down the total rolling power consumption into distinct components, each calculated separately and then aggregated, ensuring a more detailed and accurate assessment.
2) Additional power consumption estimation: A method for calculating the power consumption of equipment other than the major motors is proposed. By using the main motor power model and real-time data, this approach enables the estimation of additional power consumption, addressing the challenge of measuring these values directly on-site.
3) Power consumption prediction: we develop models to predict the rated power consumption of rough and finishing rolling motors by combining data-driven methods with mechanistic models. This integration leverages historical data while incorporating physical process insights, which enhances the prediction accuracy and reliability.

The rest of this paper is structured as follows. In Section 2, we analyze the power consumption distribution of medium and thick plate rolling and give the relevant mechanism model; In Section 3, we propose a rolling power consumption calculation algorithm based on the time slicing method; In Section 4, we give a comprehensive rolling power consumption prediction method that integrates mechanism and data, including rolling force estimation, data set creation, data preprocessing, model training, etc.; In Section 5, we provide is an experimental verification of the method in this paper; In Section 6, we summarize this paper and look to future work.

2. Electricity consumption distribution and related models of medium and thick plate rolling

The electricity consumption of medium and thick plate rolling is relatively complex, mostly including the power consumption of the main motor and the power consumption of many auxiliary systems and equipment. This section, we analyze the distribution of power consumption and give the main motor power model and SIMS rolling force model, which provides a basis for the subsequent calculation and prediction algorithm design.

2.1. Electricity consumption distribution of medium and thick plate rolling

The rolling process of medium and thick plates is complex, and common links include rough rolling, finishing rolling, cooling, straightening, etc. (as shown in Figure 1). The power consumption of the rolling process is mainly concentrated on the energy consumption of the main rolling mill drive motor, especially the power consumption of the rough rolling motor and the finishing rolling motor. These two motors have key tasks in the rolling process: The rough rolling motor is responsible for the initial compression and molding of the original billet, consuming a large amount of energy to overcome the high initial deformation resistance of the material; and the finishing rolling motor further accurately controls the thickness, surface quality, and dimensional tolerance of the steel. The proportion of the main motor power consumption in the total power consumption of the rolling process is often as high as 60% to 80%, depending on the type of rolling process, equipment configuration, and production conditions.

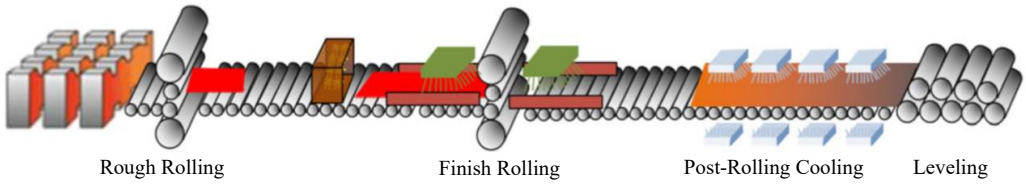


Figure 1. Plate rolling process.

Although the power consumption of the auxiliary systems in the rolling process is relatively small compared to the energy consumption of the main rolling mill drive motor, it accounts for a certain proportion in the rolling process, usually accounting for 20% to 40% of the total power consumption. The power consumption of these auxiliary systems includes:

- Power consumption of hydraulic system: It is mainly responsible for assisting the rolling mill in roller adjustment, replacement, and other auxiliary operations. Its operating power consumption accounts for a certain proportion in the rolling process.
- Power consumption of the cooling system: During the rolling process, the cooling system is used to reduce the temperature of the steel to ensure its surface quality and mechanical properties. Usually, a water cooling or air cooling system is used, and its power consumption depends on the cooling method and frequency.
- Lubrication system power consumption: In order to reduce the friction between the material and the rollers during the rolling process, the lubrication system needs to consume electrical energy to transport and maintain the supply lubricant.

- Power consumption of the conveying system: Responsible for conveying billets and finished products between different processes in the rolling process.

In addition to the power consumption of the main motor and the auxiliary system, the power consumption of the rolling process also includes power losses in the power system. Power losses mainly occur in the process of power transmission, conversion, and distribution, involving energy losses in transformers, cables, power grids, and other electrical equipment. These losses include transmission losses (heat losses caused by cable resistance), voltage transformation losses (energy losses generated by transformers during voltage conversion), and electrical losses in other equipment. It usually accounts for 5% to 10% of the total power consumption, but the cumulative effect cannot be ignored in high-load, long-term rolling processes.

All power consumption in the medium and thick plate rolling process is called rolling comprehensive power consumption, referred to as rolling power consumption; the power consumption of the rough rolling motor and the finishing rolling motor is called the main motor power consumption, referred to as the main power consumption; and the power consumption of the auxiliary system is also referred to as the auxiliary power consumption. The distribution and proportion of each power consumption are shown in Figure 2.

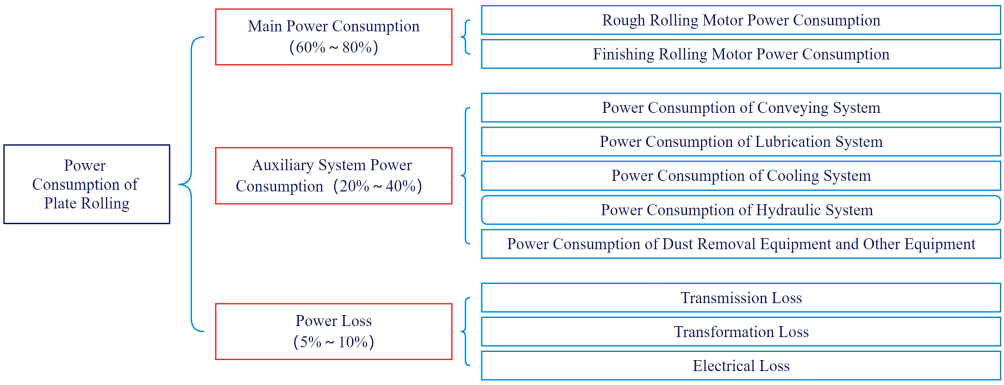


Figure 2. Distribution of power consumption in plate rolling.

2.2. Power model of rolling main motor

As shown in the Figure 3 [17], when the workpiece is not subjected to other external forces, the normal forces N_1 and N_2 of the workpiece on the two rollers and the resultant forces P_1 and P_2 of the friction forces T_1 and T_2 must be equal in magnitude and opposite in direction, and act on a straight line. Therefore, the rolling torque required to rotate the rollers is

$$M_1 = M_2 = Pa = Pl_c\psi. \tag{1}$$

The total rolling torque is

$$M_p = 2Pa = 2Pl_c\psi, \tag{2}$$

where P, a, ψ, and M represent rolling force, lever arm, lever arm coefficient, and rolling moment, respectively.

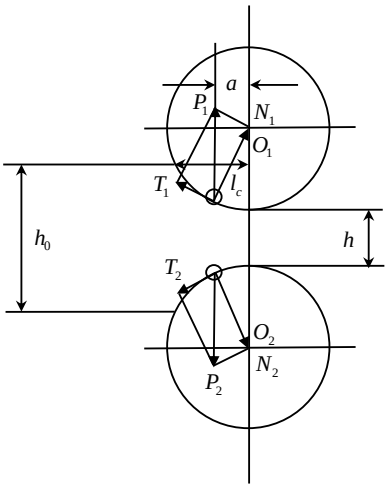


Figure 3. Rolling force diagram.

The arm coefficient is related to the geometry of the deformation zone l_c/h_m and the friction coefficient μ. The larger the l_c/h_m and μ, the smaller the ψ value. However, for simple calculations, $\psi = 0.5$ is often used. Thus

$$M_p = 2Pl_c\psi = Pl_c. \tag{3}$$

The rolling power is defined as the product of the rolling torque and the angular velocity

$$Q = M_p\omega. \tag{4}$$

The relationship between angular velocity ω and rotation speed n is

$$\omega = \frac{2\pi n}{60}. \tag{5}$$

Substituting (5) into (4) and converting the W obtained from (4) to kW, we have

$$Q = \frac{M_p n}{9550}, \tag{6}$$

where Q, ω and n represent rolling power, roll angular velocity, and roll speed, respectively.

2.3. SIMS rolling force model

The SIMS rolling force model (Simmons formula) is a classic formula in the hot rolling process [18]. The rolling force is generated due to the plastic deformation of the material between the rollers. We need to make some basic assumptions about the rolling process: During hot rolling, the material is in a state of plastic deformation, and the flow stress σ_f can be replaced by the yield stress σ_s.

As shown in Figure 3, during the rolling process, the force exerted by the roll on the roll is achieved by the plastic deformation of the material. The larger the contact area A, the greater the rolling force F required, as the stress distribution on the contact surface creates greater resistance to the flow of the material. The larger flow stress σ_f is the stronger the resistance to deformation of the material, and correspondingly, the rolling force will also increase, which can be expressed as:

$$F = \sigma_f \cdot A, \tag{7}$$

where the contact area A is defined as the product of the width of the rolled piece b and the contact arc length l_c. The contact arc length l_c is determined by the roller radius R and the reduction amount $\Delta h = \frac{h_0 - h}{2}$, and can be approximately calculated as:

$$l_c = \sqrt{R \cdot \Delta h}. \tag{8}$$

Substituting the expression of the contact area A into (7), we get:

$$F = \sigma_f \cdot b \cdot \sqrt{R \cdot \Delta h}. \tag{9}$$

The rolling force is not only affected by the rheological characteristics of the material, but also related to the geometric relationship between the roll radius R and the initial rolling thickness h_0. In the hot rolling process, the radius of the roll determines the geometry of the contact area, so it has a direct impact on the magnitude of the rolling force. By studying the relationship between roll geometry and rolling force, we found that the ratio between flow stress and roll radius R has a significant impact on rolling force.

Based on the above analysis, the SIMS formula (Simmons formula) is used to calculate the rolling force during hot rolling:

$$F = K \cdot b \cdot \Delta h \cdot (\sigma_s + \sigma_f \cdot \frac{R}{h_0}). \tag{10}$$

Here, σ_s represents yield stress, and h_0 represents initial rolling thickness. Substituting σ_f with σ_s yields the final expression for rolling force:

$$F = K \cdot b \cdot \Delta h \cdot \sigma_s \cdot (1 + \frac{R}{h_0}). \tag{11}$$

The units of the above parameters and variables are given in Table 1.

Table 1. Units of parameters or variables in power model and rolling force model.

Symbol	N_1,N_2,T_1,T_2,P_1,P_2	l_c,a,b,Δh,R,h_0	M_p	Q	ω	n	σ_s	ψ, C
Unit	kN	m	kN·m	kW	rad/s	r/min	MPa	—

3. The rolling power consumption accounting algorithm based on time slicing method

This section, we introduce the concept of time slicing, propose a power consumption calculation method for typical rolling links, and give a comprehensive power consumption calculation algorithm for billets during rolling. On this basis, combined with the main motor power model, a method for calculating the additional power consumption of major motors that are difficult to calculate directly is provided.

3.1. The idea of the time slicing method

The basic principle of the time slicing method is to record the power consumption data of the equipment at a specific time point during the production process to capture the energy consumption

changes of the equipment in each operation stage. By accurately collecting and calculating the power consumption data in these time periods, the energy consumption of the equipment under different working conditions can be analyzed.

The advantage of the time slicing method is that it can correspond the operating status of the equipment with the power consumption, gradually refine the monitoring of energy consumption, and make energy use more transparent. For example, by recording and analyzing the power consumption in different operation stages such as standby, load and no-load, the time slicing method can comprehensively track the energy consumption distribution of the equipment in the production process. In addition, the time slicing method is highly flexible and adaptable. Not only can it be used for instantaneous energy consumption monitoring in a short period of time, but it also provide reliable data support for energy consumption trend analysis and energy efficiency optimization through long-term monitoring accumulation.

The following is the time slicing method accounting process for five typical links: Rough rolling, finishing rolling, cooling, straightening, and transmission. Similar processing can be performed for other auxiliary processes or special processes. The electricity consumed by these five links is represented by E_1, E_2, E_3, and E_4, respectively.

1) Energy consumption calculation of rough rolling

During the repetitive rolling process of the medium and thick plate mill, since each piece of rolled product passes through the mill independently, the tracking system can obtain the rolling information of each piece of rolled product in real time, so as to accurately calculate its energy consumption. When the slab enters the mill, the tracking system first obtains the number of the slab through the sensor, which is used to uniquely identify the slab, ensuring that each slab can be accurately tracked in the subsequent energy consumption calculation. The system also synchronously obtains the rolling pass information, which is the identification of each time the slab passes through the mill during the rolling process. The most important thing is that the sensor will generate a steel bite signal at the moment when the slab is bitten by the mill. These steel bite signals and related time points are the basis for the subsequent calculation of the power consumption of each pass.

Assume that there are O_1 passes in the rough rolling process. For the power consumption of a single pass, let the start time be $t_{1,i}^{\text{start}}$ and the end time be $t_{1,i}^{\text{end}}$. Record the meter readings $E_{1,i}^{\text{start}}$, $E_{1,i}^{\text{end}}$ at the two times respectively. Then, the power consumption $E_{1,i}$ of this pass can be expressed as:

$$E_{1,i} = E_{1,i}^{\text{end}} - E_{1,i}^{\text{start}}, \quad i = 1, 2, \ldots, O_1. \tag{12}$$

During the rolling process, it takes a certain amount of time for the steel plate to be thrown out and returned, so there is a time interval between each pass. Similar to the process of obtaining (12), the power consumption of each pass interval time $E_{1,i}^{\text{gap}}$ can be obtained, which can be expressed as:

$$E_{1,i}^{\text{gap}} = E_{1,i+1}^{\text{start}} - E_{1,i}^{\text{end}}, \quad i = 1, 2, \ldots, O_1 - 1. \tag{13}$$

In summary, according to (12) and (13), the power consumption of the slab in the rough rolling process can be obtained:

$$E_1 = \sum_{i=1}^{O_1} (E_{1,i} + E_{1,i}^{\text{gap}}), \tag{14}$$

where $E_{1,O_1}^{\text{gap}} = 0$.

2) Energy consumption calculation in finishing rolling

The energy consumption calculation method of the finishing rolling stage is similar to that of the rough rolling stage. Assume that there are O_2 passes in the finishing rolling process. For the power consumption of a single pass, the start time of the pass is $t_{2,i}^{\text{start}}$, and the end time is $t_{2,i}^{\text{end}}$. The corresponding readings of the electric meter at these two times are $E_{2,i}^{\text{start}}$ and $E_{2,i}^{\text{end}}$. Then, the power consumption $E_{2,i}$ of this pass can be expressed as:

$$E_{2,i} = E_{2,i}^{\text{end}} - E_{2,i}^{\text{start}}, \quad i = 1, 2, \ldots, O_2. \tag{15}$$

The power consumption during the interval between passes $E_{2,i}^{\text{gap}}$ can be expressed as:

$$E_{2,i}^{\text{gap}} = E_{2,i+1}^{\text{start}} - E_{2,i}^{\text{end}}, \quad i = 1, 2, \ldots, O_2 - 1. \tag{16}$$

Combining (15) and (16), the power consumption of the finishing rolling process can be obtained:

$$E_2 = \sum_{i=1}^{O_2} (E_{2,i} + E_{2,i}^{\text{gap}}), \tag{17}$$

where $E_{2,O_2}^{\text{gap}} = 0$.

3) Energy consumption calculation of the straightening process

During the rolling process of medium and thick plates, the straightening process is usually completed in one step to ensure that the flatness and geometric dimensions of the slab meet the quality standards. Usually only one slab is operated in each straightening link to accurately control the straightening process. However, if the flatness or dimensional accuracy of the slab does not meet the requirements after the first straightening, multiple straightenings may be required until the slab meets the specified standards. The purpose of multiple straightenings is to correct defects such as warping or bending generated during the rolling process to ensure that the final product has good flatness and dimensional accuracy to meet customer requirements.

At the beginning and end of each slab straightening process, record the meter readings $E_{3,i}^{\text{start}}$, $E_{3,i}^{\text{end}}$, $i = 1, 2, \ldots, O_3$, where O_3 represents the total number of straightening times. From this, the power consumption of the straightening link can be obtained:

$$E_3 = \sum_{i=1}^{O_3} (E_{3,i}^{\text{end}} - E_{3,i}^{\text{start}}), \quad i = 1, 2, \ldots, O_3. \tag{18}$$

4) Energy consumption calculation of the slab transport process

According to the calculation process of the above time slice method, we can record the number of slabs transmitted and the power consumption within a certain time period, and thus calculate the power consumption of the slab per unit mass and unit length E_{cell}. Let the total transmission length of the slab during the rolling process be L, then the transmission power consumption of the slab can be obtained as:

$$E_4 = E_{\text{cell}} \cdot m \cdot L, \tag{19}$$

where m represents the mass of the slab.

In summary, according to (14), (17)–(19), the power consumption E of the slab during the entire rolling process can be calculated:

$$E = E_1 + E_2 + E_3 + E_4. \tag{20}$$

3.2. Algorithm implementation

The method in the previous section is used to calculate the total power consumption of the rolling process, including the energy consumption of the roughing and finishing passes, the energy consumption of the cooling process, the energy consumption of the straightening process, and the power consumption during the transmission process. By accumulating the energy consumption of each stage pass by pass, the time interval between each pass is taken into account, so as to more accurately reflect the power consumption of the rolling process. In addition, by calculating the cooling and straightening processes separately, it is ensured that the energy consumption of each link is fully evaluated to obtain the total power consumption of the entire rolling process.

The implementation of the entire method can be summarized as Algorithm 1, which contains the input variables shown in Table 2.

Algorithm 1: Rolling power consumption accounting algorithm based on time slicing method

Input: Input variables shown in Table 2

Output: Total power consumption E of the entire rolling process

begin
  for $i \leftarrow 1$ **to** O_1 **do**
    Calculate the power consumption of each rough rolling pass $E_{1,i}$;
    if $i < O_1$ **then**
      Calculate the power consumption of the rough rolling pass interval $E_{1,i}^{\text{gap}}$;
    else
      If it is the last pass, the power consumption of the time interval is set to 0, that is, $E_{1,O_1}^{\text{gap}} = 0$;
    The power consumption of the current pass and its interval is added to E_1;
  for $i \leftarrow 1$ **to** O_2 **do**
    According to (15), the power consumption of each finishing pass is calculated as $E_{2,i}$;
    if $i < O_2$ **then**
      According to (16), the power consumption of the finishing pass interval is calculated as $E_{2,i}^{\text{gap}}$;
    else
      If it is the last pass, the power consumption of the time interval is set to 0, that is, $E_{2,O_2}^{\text{gap}} = 0$;
    Add the power consumption of the current pass and its interval to E_2;
  for $i \leftarrow 1$ **to** O_3 **do**
    According to (18), calculate the power consumption of each straightening $E_{3,i}$;
    Add the current straightening power consumption to E_3;
  According to (19), calculate the power consumption of the slab transmission process E_4;
  According to (20), calculate the total power consumption E of the entire rolling process.

Table 2. Algorithm 1 input variables.

Variable	Symbol
Pass counts for roughing, finishing, and straightening	O_1,O_2,O_3
Start and end times of rough and finish passes	$t_{1,i}^{\text{start}}$, $t_{1,i}^{\text{end}}$, $t_{2,i}^{\text{start}}$, $t_{2,i}^{\text{end}}$
Electric meter readings at start/end of rough/finish passes	$E_{1,i}^{\text{start}}$, $E_{1,i}^{\text{end}}$, $E_{2,i}^{\text{start}}$, $E_{2,i}^{\text{end}}$
Meter readings before/after i-th straightening	$E_{3,i}^{\text{start}}$, $E_{3,i}^{\text{end}}$
Power per unit mass and length of slab	E_{cell}
Slab mass	m
Slab length	L

3.3. Calculation of additional power consumption of main motor

In the previous section, we present the comprehensive power consumption of a billet during rolling. In contrast, the rated power consumption of the main motor can be determined based on the set parameters for rough rolling and finishing rolling, as well as the billet's rolling process. By subtracting the rated power consumption of the main motor from the total power consumption (as shown in Figure 4), we obtain the power consumption beyond the rated value of the main motor for rough rolling and finishing rolling. This is referred to as the "additional power consumption", which includes the auxiliary system's power consumption, power losses during the rolling process, and the power consumption deviation of the main motor (i.e., the difference between actual and rated power consumption).

Calculating additional power consumption is inherently difficult due to its complex and dispersed nature, involving auxiliary devices and power losses. Moreover, frequent changes in operational conditions, challenges in energy consumption allocation, difficulty in measuring hidden losses, and the lack of precise measurement tools and models further complicate its accurate estimation. As a result, indirect methods are typically the only feasible approach to calculate this additional power consumption.

In the following sections, we calculate the rated power consumption of the main motor for rough and finishing rolling. The calculation method for the additional power consumption is then proposed, building on the approach introduced in the previous section. The additional power consumption of the main motor is denoted as E_e.

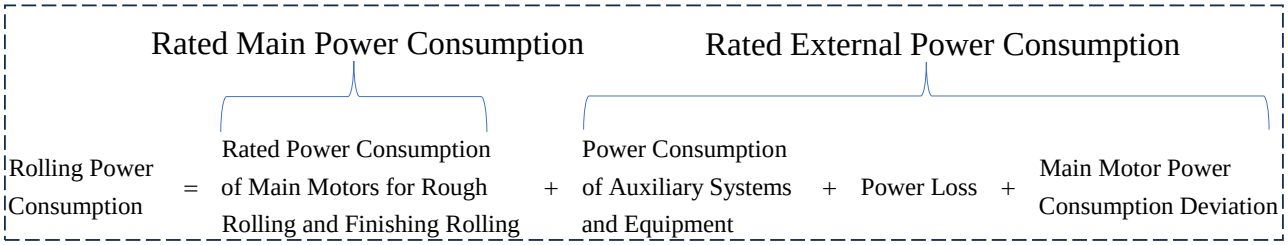


Figure 4. Composition of rolling power consumption.

The power consumption of the main motor is the main energy consumption part in the rolling process. The rolling power can be calculated based on the power model. Combined with the law of conservation of energy and (6) and the steel biting and throwing signals, the rated power consumption

of a certain rolling pass of the steel billet in the rough rolling process can be obtained:

$$W_1^i = Q_1(t_{1,i}^{\text{end}} - t_{1,i}^{\text{start}}) = \frac{1}{3600}\frac{M_{P1}^i n_1}{9550\eta_1}(t_{1,i}^{\text{end}} - t_{1,i}^{\text{start}}), \quad i = 1, 2 \ldots, O_1. \tag{21}$$

Similarly, the power consumption W_2^i of each pass of finishing rolling is:

$$W_2^i = Q_2(t_{2,i}^{\text{end}} - t_{2,i}^{\text{start}}) = \frac{1}{3600}\frac{M_{P2}^i n_2}{9550\eta_2}(t_{2,i}^{\text{end}} - t_{2,i}^{\text{start}}), \quad i = 1, 2 \ldots, O_2. \tag{22}$$

In (21) and (22), Q_i, M_{Pi}^i, n_i, η_i represent motor power, rolling torque, roller speed, and motor efficiency, respectively. When $i = 1$, it represents the parameters of the rough rolling main motor, and when $i = 2$, it represents the parameters of the finishing rolling main motor.

In each rolling process, the roller speed will drop only at the moment of biting the steel. After entering the rolling state, the roller speed remains approximately unchanged. The roller speed can be obtained based on the roller linear speed v_1 and the roller radius R_1 during rough rolling.

$$n_1 = \frac{30v_1}{\pi R_1}. \tag{23}$$

Similarly, the roller speed during finishing rolling

$$n_2 = \frac{30v_2}{\pi R_2}. \tag{24}$$

Substitute (23) and (24) into (21) and (22) respectively, and then add the power consumption of each pass and the power consumption of rough rolling and finish rolling to obtain the rated power consumption W of the main motor:

$$\begin{aligned} W &= \sum_{i=1}^{O_1} W_1^i + \sum_{i=1}^{O_2} W_2^i \\ &= \frac{1}{120}\sum_{i=1}^{O_1} \frac{M_{P1}^i v_1}{9550\eta_1\pi R_1}(t_{1,i}^{\text{end}} - t_{1,i}^{\text{start}}) + \frac{1}{120}\sum_{i=1}^{O_2} \frac{M_{P2}^i v_2}{9550\eta_1\pi R_2}(t_{2,i}^{\text{end}} - t_{2,i}^{\text{start}}). \end{aligned} \tag{25}$$

Based on the above, we can obtain the additional power consumption of the main motor $E_e = E - W$, where E is given by (20) and W is given by (25).

4. A mechanism- and data-driven algorithm the rolling power consumption

This section, we propose a rolling power consumption prediction method that integrates mechanism and data. First, we describe our thinking framework; then, we use the rolling force model and power model to calculate the rated power consumption of the main motor; then, we use the data model to predict other power consumption that is difficult to describe with mechanism; finally, the algorithm is implemented.

4.1. Thinking framework

During the rolling process, the power consumption of the main motor is the core part of the power consumption, which is mainly generated when the roller system applies pressure to the billet. Since the working mechanism of the main motor is relatively clear, it can be calculated through the rolling power model according to parameters such as rolling force, roller speed, and billet size. However, this calculation obtains the power consumption under the rated working state, and there will inevitably be certain deviations due to changes in conditions in working conditions.

In contrast, the auxiliary power consumption of other systems and equipment other than the main motor is more complicated. The energy consumption of these systems is closely related to multiple factors such as process conditions, equipment status, and operation mode. It is difficult to accurately calculate with simple physical formulas, and it cannot be directly calculated through a certain physical model like the power consumption of the main motor.

In addition, the power loss in the rolling process is also difficult to accurately calculate through the mechanism model. The power loss is affected by dynamic process parameters, and there is a complex nonlinear relationship between these parameters. In addition, uncertain factors such as equipment wear, changes in material properties and environmental fluctuations are difficult to quantify, making accurate modeling more difficult.

To solve this problem, we consider the main motor power consumption deviation, auxiliary system power consumption, and power loss as a whole, and use a data-driven approach to predict based on historical production data, inspired by some system identification methods [19,20]. We use the random forest algorithm to learn the relationship between features, such as billet size and rolling pass information and the main motor's additional power consumption, and build a main motor additional power consumption prediction model.

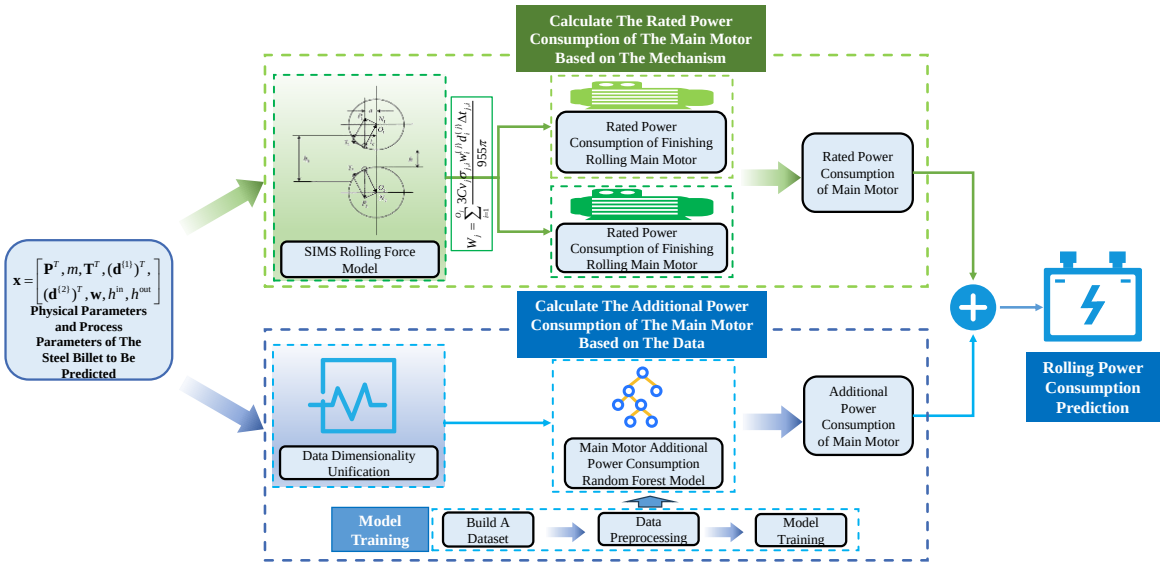


Figure 5. The framework of rolling power consumption prediction based on mechanism and data fusion.

Based on these considerations, we propose a prediction method of mechanism and data fusion. For the rated power consumption of the main motor of rough rolling and finishing rolling, the SIMS

rolling force model is used for calculation. For other power consumption other than the rated power consumption of the main motor, a model based on data training is used for calculation. As shown in Figure 5, the specific implementation steps are as follows:

Step 1: Calculate the rated power consumption of the main motor For rough rolling and finishing rolling, first calculate the rolling force, then calculate the power, and then get the rated power consumption of the main motor;

Step 2: Predict the additional power consumption of the main motor First, establish a data set and unify the dimension of the input vector; then, train the random forest model of the additional power consumption of the main motor; and then give the predicted value of the additional power consumption of the main motor that needs to be predicted for the billet;

Step 3: Give the rolling power consumption of the steel plate Add the results of the first and second steps to give the predicted value of the rolling power consumption of the billet.

Based on the above ideas, the power consumption of a billet during rolling is predicted, and its physical parameters and process parameters are recorded as

$$\mathbf{x} = \left[\begin{array}{ccccccc} \mathbf{p}^T & m & \mathbf{T}^T & (\mathbf{d}^{\{1\}})^T & (\mathbf{d}^{\{2\}})^T & \mathbf{w} & h^{\text{in}} \quad h^{\text{out}} \end{array} \right]. \tag{26}$$

In the above formula, the meaning of each element in $\mathbf{x}$ is the same as the meaning of each element in $\mathbf{x}_i$ in (40). Below, $\hat{E}(\mathbf{x})$ and $\hat{E}_e(\mathbf{x})$ are used to represent the rolling power consumption prediction value of the steel plate $\mathbf{x}$ and the additional power consumption prediction value of the main motor, respectively.

4.2. Calculation of rated power consumption of the main motor

During the rolling process of medium and thick plates, the thickness of the slab will decrease as the rolling passes increase, and the temperature will gradually decrease as the process progresses. The yield stress characteristics of steel materials at different temperatures are also different. At high temperatures, the yield stress of steel is low, which facilitates plastic deformation; as the temperature decreases, the atomic motion inside the steel weakens, the crystal structure becomes more stable, the yield stress increases, and the material becomes more difficult to deform. This dynamic change of temperature and yield stress has a significant impact on the power consumption of the rolling process.

The rated power consumption of the main motor in the rough rolling and finishing rolling of the billet $\mathbf{x}$ is calculated below. During the rolling process, assume that the change curve of slab temperature with time is expressed as $T = \text{Tem}(t)$, and the change curve of yield stress with slab temperature is $\sigma = \text{Str}(T)$*.

1) Rated power consumption of the main motor for rough rolling

The volume of the slab does not change much during the rolling process, so the volume can be considered to be conserved.

$$L_{1,i} \cdot w_i^{\{1\}} \cdot \left[h_i^{\text{in}} - \sum_{j=0}^{i} d_j^{\{1\}} \right] = L_{1,i+1} \cdot w_{i+1}^{\{1\}} \cdot \left[h_i^{\text{in}} - \sum_{j=0}^{i+1} d_j^{\{1\}} \right], \quad i = 0, 1, 2, \ldots, O_1 - 1, \tag{27}$$

where $L_{1,i}$ and $w_i^{\{1\}}$ represent the length and width of the steel plate at the end of the $(i-1)$th rolling pass. When $i = 0$, that is, $L_{1,0}$ and $w_0^{\{1\}}$ represent the length of the slab before rough rolling; $d_0^{\{1\}} = 0$.

*The change curve of billet temperature with time and the change curve of yield stress with temperature can usually be obtained by experimental measurement, numerical simulation, theoretical calculation or empirical formula, or a combination of these methods.

From this, we can get the slab length at the end of the ith pass

$$L_{1,i+1} = \frac{L_{1,i} \cdot w_i^{\{1\}} \cdot \left[h_i^{\text{in}} - \sum_{j=0}^{i+1} d_j^{\{1\}}\right]}{w_{i+1}^{\{1\}} \cdot \left[h_i^{\text{in}} - \sum_{j=0}^{i} d_j^{\{1\}}\right]}, \quad i = 0, 1, 2, \ldots, O_1 - 1. \tag{28}$$

According to the roller linear speed v_1 and the length of the slab after rolling $L_{1,i+1}$, the rolling time of each pass can be obtained:

$$\Delta t_{1,i} = \frac{L_{1,i+1}}{v_1}, \quad i = 0, 1, 2, \ldots, O_1 - 1. \tag{29}$$

T_s represents the starting temperature of rough rolling, and $t_1 = \text{Tem}^{-1}(T_s)$ is set. Substitute $t_1 + \sum_{k=1}^{1} \Delta t_{1,1}, t_1 + \sum_{k=1}^{2} \Delta t_{1,2}, \ldots, t_1 + \sum_{k=1}^{O_1} \Delta t_{1,O_1}$ into $T = \text{Tem}(t)$, and we can get the temperature of the slab at the end of each pass, $T_{1,1}, T_{1,2}, \ldots, T_{1,O_1}$. The whole solution process is shown in Figure 6. Substituting T_s and these temperatures into $\sigma = \text{Str}(T)$, we can obtain the yield strength $\sigma_{1,1}, \sigma_{1,2}, \ldots, \sigma_{1,O_1}$ in each pass.

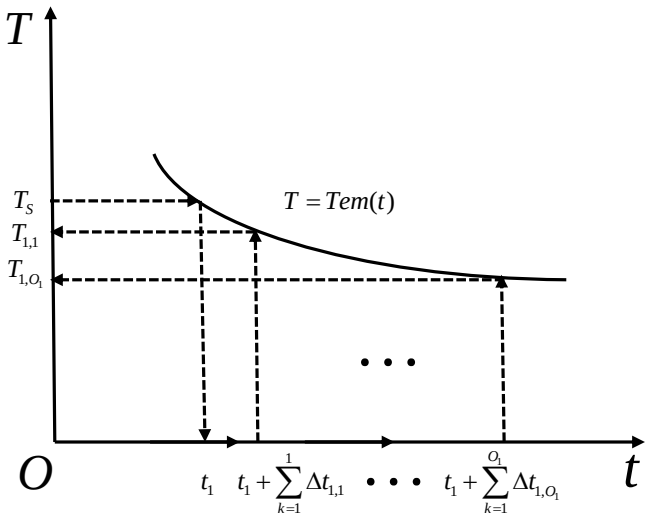


Figure 6. The process of calculating the temperature of the billet during the rough rolling process.

According to (11), the rolling force of each pass of rough rolling can be obtained:

$$F_{1,i} = K d_i^{\{1\}} \sigma_{1,i} w_i^{\{1\}} \left(1 + \frac{R_1}{h_{0,i}^{\{1\}}}\right). \tag{30}$$

Then, the rolling moment of each rough rolling pass is obtained: $M_{1,i} = F_{1,i} l_{1,i}$, where $l_{1,i}$ is the horizontal projection length of the contact arc, which can be calculated by the following formula:

$$l_{1,i} = \sqrt{R_1 d_i^{\{1\}}}, \quad i = 1, 2, \ldots, O_1. \tag{31}$$

According to (4) and (6), the rated power consumption of the main motor during the rough rolling process of the entire slab can be obtained:

$$W_1 = \sum_{i=1}^{O_1} \frac{3K v_1 d_i^{\{1\}} \sigma_{1,i} w_i^1 (h_{0,i}^{\{1\}} + R_1) \sqrt{R_1 d_i^{\{1\}}} \Delta t_{1,i}}{955 \pi R_1 h_{0,i}^{\{1\}}}. \tag{32}$$

2) Rated power consumption of finishing rolling main motor

Similar to (27), we can get

$$L_{2,i} \cdot w_i^{\{2\}} \cdot \left[h_i^{\text{out}} + \sum_{j=0}^{i} d_j^{\{2\}} \right] = L_{2,i+1} \cdot w_{i+1}^{\{2\}} \cdot \left[h_i^{\text{out}} + \sum_{j=0}^{i+1} d_j^{\{2\}} \right], \quad i = O_2 - 1, O_2 - 2, \ldots, 1, 0. \tag{33}$$

where $L_{2,i}$ and $w_i^{\{2\}}$ represent the length and width of the steel plate at the end of the $(i-1)$th rolling pass. When $i = 0$, that is, $L_{2,0}$ and $w_0^{\{2\}}$ represent the length of the slab after finish rolling; $d_0^{\{2\}} = 0$. Thus, the length of the slab at the end of the ith rolling pass can be obtained.

$$L_{2,i+1} = \frac{L_{2,i+1} L_{2,i} \cdot w_i^{\{2\}} \cdot \left[h_i^{\text{out}} + \sum_{j=0}^{i-1} d_j^{\{2\}} \right]}{w_{i+1}^{\{1\}} \cdot \left[h_i^{\text{out}} + \sum_{j=0}^{i} d_j^{\{2\}} \right]}, \quad i = O_2 - 1, O_2 - 2, \ldots, 1, 0. \tag{34}$$

Thus, the rolling time for each pass can be obtained:

$$\Delta t_{2,i} = \frac{L_{2,i+1}}{v_2}, \quad i = O_2 - 1, O_2 - 2, \cdots, 1, 0, \tag{35}$$

where v_2 represents the linear velocity of the roller.

T_e represents the final rolling temperature at the end of finishing rolling, and $t_2 = \text{Tem}^{-1}(T_e)$ is set. Substitute $t_2 - \sum_{k=1}^{1} \Delta t_{2,1}, t_1 - \sum_{k=1}^{2} \Delta t_{21,2}, \ldots, t_1 - \sum_{k=1}^{O_2} \Delta t_{2,O_2}$ into $T = \text{Tem}(t)$, then the temperature of the slab at the end of each rolling pass can be obtained, T_{2,O_2-1}, T_{2,O_2-2}, …, $T_{2,1}$, the solution process is shown in Figure 7. Substituting T_e and these temperatures into $\sigma = \text{Str}(T)$, we can obtain the yield strength $\sigma_{2,O_2}, \sigma_{2,O_2-1}, \ldots, \sigma_{2,1}$ in each pass.

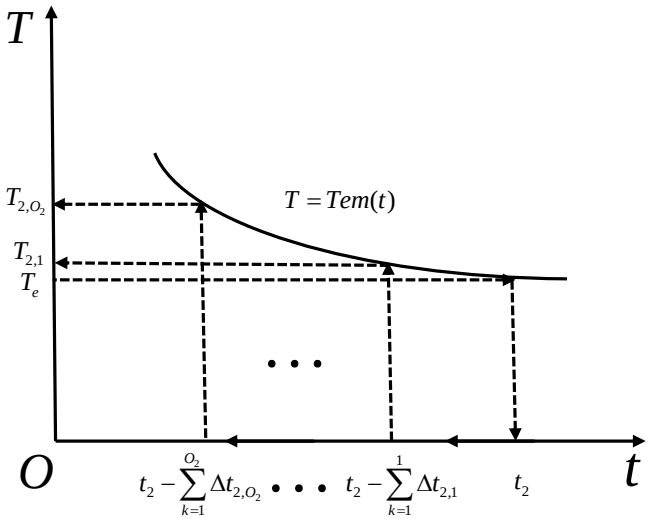


Figure 7. The process of calculating the temperature of the steel billet during the finishing rolling process.

According to (11), the rolling force of each pass of finishing rolling can be obtained:

$$F_{2,i} = K d_i^{\{2\}} \sigma_{1,i} w_i^{\{2\}} (1 + \frac{R_2}{h_{0,i}^{\{2\}}}). \tag{36}$$

Furthermore, the rolling moment of each pass of finishing rolling can be obtained as $M_{2i} = F_{2i}l_{2i}$, where l_{2i} is the horizontal projection length of the contact arc, which can be calculated by the following formula:

$$l_{2,i} = \sqrt{R_2 d_i^{\{2\}}}, \quad i = 1, 2, \ldots, O_2. \tag{37}$$

According to (4) and (6), the rated power consumption of the main motor during the slab finishing rolling process can be obtained:

$$W_2 = \sum_{i=1}^{O_2} \frac{3Kv_2 d_i^{\{2\}} \sigma_{2,i} w_i^2 (h_{0,i}^{\{2\}} + R_2) \sqrt{R_2 d_i^{\{2\}}} \Delta t_{2,i}}{955\pi R_2 h_{0,i}^{\{2\}}}. \tag{38}$$

Finally, the rated total power consumption of the main motor during the slab rolling process can be obtained:

$$\begin{aligned} W &= W_1 + W_2 \\ &= \sum_{i=1}^{O_1} \frac{3Kv_1 d_i^{\{1\}} \sigma_{1,i} w_i^1 (h_{0,i}^{\{1\}} + R_1) \sqrt{R_1 d_i^{\{1\}}} \Delta t_{1,i}}{955\pi R_1 h_{0,i}^{\{1\}}} + \sum_{i=1}^{O_2} \frac{3Kv_2 d_i^{\{2\}} \sigma_{2,i} w_i^2 (h_{0,i}^{\{2\}} + R_2) \sqrt{R_2 d_i^{\{2\}}} \Delta t_{2,i}}{955\pi R_2 h_{0,i}^{\{2\}}}, \end{aligned} \tag{39}$$

Among them, $\Delta t_{1,i}$ and $\Delta t_{2,i}$ are given by (29) and (35) respectively.

4.3. Prediction of additional power consumption of main motor

4.3.1. Construction the of training dataset for the prediction model

The power consumption of steel billets during the rolling process is influenced by a variety of factors, including the billet's physical properties and the precise control of the rolling process. From a material perspective, factors such as chemical composition, thickness, and weight directly affect the hardness of the steel billet. Steel billets with different chemical compositions exhibit significant variations in hardness, and higher hardness requires greater rolling pressure and energy consumption. Additionally, the thickness and weight of the billet impact energy consumption as well—thicker or heavier billets generally require more energy to achieve the desired deformation.

From a process perspective, the rolling schedule plays a critical role in determining energy consumption, particularly the number of rolling passes and the reduction per pass. The reduction in each pass directly influences the depth and intensity of the deformation, with larger reductions leading to higher energy consumption. Moreover, both the initial and final rolling temperatures significantly affect energy usage. A higher initial rolling temperature can reduce the hardness of the billet, lowering energy requirements for rolling. In contrast, controlling the final rolling temperature is crucial for both the quality of the final product and the energy consumed during the process.

Taking the above into consideration, we construct a training data set $\mathcal{D}$ for the additional power consumption prediction model, and each element of the data set represents the correspondence between the physical parameters and process parameters of a steel billet and the additional power consumption of the main motor. Denote $\mathcal{D} = \{D_1, D_2, \ldots, D_n\}$, where $D_i = (\mathbf{x}_i, y_i)$, y_i is used as model output, represents the additional power consumption of the main motor during the billet rolling process; $\mathbf{x}_i$ is used as model input, as follows:

$$\mathbf{x}_i = \left[\begin{array}{ccccccc} \mathbf{p}_i^T & m_i & \mathbf{T}_i^T & (\mathbf{d}_i^{\{1\}})^T & (\mathbf{d}_i^{\{2\}})^T & \mathbf{w}_i & h_i^{\text{in}} \quad h_i^{\text{out}} \end{array} \right], \tag{40}$$

where, $\mathbf{p}_i = \left[\omega(C_i), \omega(Si_i), \omega(Mn_i), \omega(P_i), \omega(S_i), \omega(Nb_i), \omega(V_i), \omega(Ti_i), \omega(Mo_i), \omega(Cr_i)\right]^T$ represents the mass fraction of carbon, silicon, manganese, phosphorus, sulfur, nickel, vanadium, titanium, molybdenum, and chromium contained in the slab; m_i represents the mass of the steel slab; $\mathbf{T}_i$ is a vector representing various temperatures specified in the rolling procedure, such as the start rolling temperature, the intermediate billet temperature, the final rolling temperature, etc. Its dimension and specific elements vary with the production line or steel type; $\mathbf{d}_i^{\{1\}} = [d_{i,1}^{\{1\}}, d_{i,2}^{\{1\}}, \ldots, d_{i,O_{i1}}^{\{1\}}]^T$ represents the reduction of each pass of rough rolling; $\mathbf{d}_i^{\{2\}} = [d_{i,1}^{\{2\}}, d_{i,2}^{\{21\}}, \ldots, d_{i,O_{i2}}^{\{2\}}]^T$ means The reduction amount of each pass of finishing rolling; $\mathbf{w}_i = [w_{i,1}^{\{1\}}, w_{i,2}^{\{1\}}, \ldots, w_{i,O_{i1}}^{\{1\}}, w_{i,1}^{\{2\}}, w_{i,2}^{\{2\}}, \ldots, w_{i,O_{i2}}^{\{2\}}]^T$ represents the set width in each pass of rough rolling and finishing rolling; h_i^{in} and h_i^{out} represent the initial thickness and target thickness respectively. The units of these variables or parameters are shown in Table 3.

Table 3. Units of parameters or variables in the training dataset of the additional power consumption prediction model.

Symbol	m_i	T_i	$\mathbf{d}_i^{\{1\}}$,$\mathbf{d}_i^{\{2\}}$,$\mathbf{w}_i$,h_i^{in},h_i^{out}	$\omega(C_i)$, $\omega(Si_i)$, …, $\omega(Ti_i)$, $\omega(Mo_i)$,$\omega(Cr_i)$
Unit	kg	°C	mm	%

Different steel grades and rolling targets often require different roughing and finishing passes, which will lead to differences in the dimensions of the pass reduction vectors $\mathbf{d}_i^1$ and $\mathbf{d}_i^2$ and the set width vector $\mathbf{w}_i$, making the dimensions of each input sample $\mathbf{x}_i$ inconsistent. This dimensional inconsistency will interfere with model training and cannot be directly input into the model, so the data must be dimensionally unified.

Assume that the maximum possible rolling passes for roughing and finishing are $\overline{O}_1$ and $\overline{O}_2$, respectively. For the case where the maximum number of passes is not reached, the missing passes can be regarded as no reduction operation (i.e., the reduction amount is 0), and the width of the missing pass is kept consistent with the width of the nearest pass, thereby filling $\mathbf{d}_i^{\{1\}}$ and $\mathbf{d}_i^{\{2\}}$ with zeros, and $\mathbf{w}_i$ is expanded using the nearest neighbor element retention method. In this way, the roughing and finishing pass reduction vectors and the set width vectors of all samples can be uniformly expanded to the same dimension, so that the dimension of each input vector is consistent. Specifically, $\mathbf{d}_i^1$, $\mathbf{d}_i^2$,and $\mathbf{w}_i$ are expanded as follows:

$$\overline{\mathbf{d}}_i^1 = [(\mathbf{d}_i^1)^T, \overbrace{0, \ldots, 0}^{\overline{O}_1 - O_{i1}}]^T, \tag{41}$$

$$\overline{\mathbf{d}}_i^2 = [(\mathbf{d}_i^2)^T, \overbrace{0, \ldots, 0}^{\overline{O}_2 - O_{i2}}]^T, \tag{42}$$

$$\overline{\mathbf{w}}_i = [w_{i,1}^{\{1\}}, \ldots, w_{i,O_{i1}}^{\{1\}}, \overbrace{w_{i,O_{i1}}^{\{1\}}, \ldots, w_{i,O_{i1}}^{\{1\}}}^{\overline{O}_1 - O_{i1}}, w_{i,1}^{\{2\}}, \ldots, w_{i,O_{i2}}^{\{2\}}, \overbrace{w_{i,O_{i2}}^{\{2\}}, \ldots, w_{i,O_{i2}}^{\{2\}}}^{\overline{O}_2 - O_{i2}}]^T. \tag{43}$$

In $\mathbf{x}_i$, $\overline{\mathbf{d}}_i^1$, $\overline{\mathbf{d}}_i^2$, and $\overline{\mathbf{w}}_i$ are used to replace $\mathbf{d}_i^1$, $\mathbf{d}_i^2$, and $\overline{\mathbf{w}}_i$, respectively, to unify the input dimensions.

To improve the stability and generalization ability of the model, it is very important to preprocess the dataset $\mathcal{D}$. Standardize or normalize the input variables and convert the data to the same dimension and scale range to avoid certain features dominating during the training process due to the difference in

variable scales, thereby reducing the bias of the model. Standardization usually transforms data into a distribution with a mean of 0 and a variance of 1, while normalization scales the data to a specific range (e.g., $[0, 1]$). In addition, there may be missing values in the dataset, which can be filled by methods such as mean filling and nearest neighbor filling.

4.3.2. Random forest prediction model establishment

Random forest is an ensemble learning algorithm proposed by Leo Breiman in 2001. It constructs multiple decision trees and combines their results to perform classification or regression prediction. It randomly extracts subsamples from the training data through "bagging" and randomly selects some features when each tree node splits to increase the difference between trees and improve the generalization ability of the model. Finally, Random forest obtains the prediction result through majority voting (classification) or averaging (regression). Random forest has the advantages of anti-overfitting, strong stability, and feature importance evaluation.

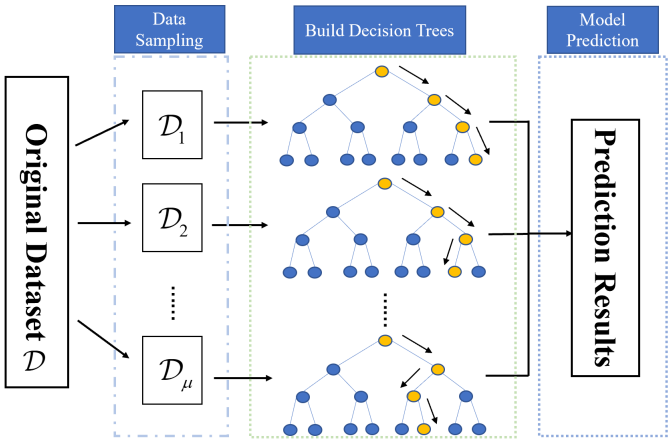


Figure 8. Random forest model building process.

As shown in Figure 8, the construction process of the random forest model can be divided into the following steps:

Step 1: data sampling

Randomly extract n samples from $\mathcal{D}$ with replacement to generate μ subsets $\mathcal{D}_j$, $j = 1, 2, \ldots, \mu$. This means that the size of $\mathcal{D}_j$ is the same as the original dataset, but contains some repeated samples.

Step 2: build a decision tree

For each sample subset $\mathcal{D}_j$, train a decision tree. Let the loss function on the decision tree node be $L_j(S)$, where S is the sample set on the current node. The mean square error is often used as the loss function:

$$L_j(S) = \frac{1}{\#(S)} \sum_{l \in S} (y_l - \bar{y})^2, \tag{44}$$

where $\bar{y}$ is the mean of all samples in node S; $\#(\cdot)$ represents the number of elements in a set.

By recursively selecting the optimal features and split points to minimize the loss function, a decision tree can be trained [21]:

- Find the optimal split feature and split point: For the candidate feature l and its split point t, divide the data set S into two subsets:

$$S_{\text{left}} = \{(\mathbf{x}_i, y_i) \in S \mid x_{il} \le t\}, \tag{45}$$

$$S_{\text{right}} = \{(\mathbf{x}_i, y_i) \in S \mid x_{il} > t\}, \tag{46}$$

  Here, x_{il} represents the lth element of $\mathbf{x}_i$. Calculate the loss function after splitting:

$$L_j(S, l, t) = \frac{\#(S_{\text{left}})}{\#(S)} L_j(S_{\text{left}}) + \frac{\#(S_{\text{right}})}{\#(S)} L_j(S_{\text{right}}). \tag{47}$$

  Select the feature l^* and split point t^* that minimizes the loss function (maximum information gain):

$$(l^*, t^*) = \arg\min_{l,t} L_j(S, l, t). \tag{48}$$

- Recursive node splitting: Repeat the above splitting process for the split child nodes S_{left} and S_{right} until the stopping condition is met (such as reaching the maximum depth, the number of node samples is less than the minimum threshold, or the node purity reaches the preset standard).
- Building leaf nodes: When the node is no longer split, set the current node as a leaf node. The output of the leaf node is the mean of all sample labels in the node:

$$\hat{y}_j = \frac{1}{\#(S)} \sum_{l \in S} y_l. \tag{49}$$

Step 3: Prediction of the integrated model

Assuming that the output of each tree is $\hat{y}_j$, the final prediction result is determined by taking the average of all tree prediction values:

$$\hat{y} = \frac{1}{\mu} \sum_{j=1}^{\mu} \hat{y}_j. \tag{50}$$

4.3.3. Prediction of additional power consumption of the main motor

According to the method given by (41)–(43), the dimensions of $\mathbf{d}^{\{1\}}$, $\mathbf{d}^{\{2\}}$ and $\mathbf{w}$ are expanded, that is,

$$\overline{\mathbf{d}}^{\{1\}} = [(\mathbf{d}^{\{1\}})^T, \overbrace{0, \ldots, 0}^{\overline{o}_1 - o_1}]^T, \tag{51}$$

$$\overline{\mathbf{d}}^{\{2\}} = [(\mathbf{d}^{\{2\}})^T, \overbrace{0, \ldots, 0}^{\overline{o}_2 - o_2}]^T, \tag{52}$$

$$\overline{\mathbf{w}} = [w_1^{\{1\}}, \ldots, w_{O_1}^{\{1\}}, \overbrace{w_{O_1}^{\{1\}}, \ldots, w_{i,O_{i1}}^{\{1\}}}^{\overline{o}_1 - o_1}, w_1^{\{2\}}, \ldots, w_{O_2}^{\{2\}}, \overbrace{w_{O_2}^{\{2\}}, \ldots, w_{O_2}^{\{2\}}}^{\overline{o}_2 - o_2}]^T. \tag{53}$$

Then, replace $\mathbf{d}^{\{1\}}$, $\mathbf{d}^{\{2\}}$, and $\mathbf{w}$ with $\overline{\mathbf{d}}^{\{1\}}$, $\mathbf{d}^{\{2\}}$, and $\mathbf{w}$ in $\mathbf{x}$.

Take $\mathbf{x}$ as the model input and bring it into the random forest model trained in Section 4.3.2, and get the predicted value of the additional power consumption of the main motor of the steel plate, $\hat{E}_e(\mathbf{x})$.

4.4. Algorithm implementation

Combining the calculated value of the rated power consumption of the main motor in Section 4.2 and the predicted value of the additional power consumption $\hat{E}_e(\mathbf{x})$ in Section 4.3.3, the predicted value of the rolling power consumption of the steel plate $\mathbf{x}$ can be obtained: $\hat{E}(\mathbf{x}) = W + \hat{E}_e(\mathbf{x})$, where W is given by (39). The implementation of the process can be summarized as algorithm 2.

Algorithm 2: Rolling comprehensive power consumption prediction algorithm

Input: Physical parameters and process parameters of the steel billet to be predicted $\mathbf{x}$
Output: Prediction value of rolling comprehensive power consumption $\hat{E}(\mathbf{x})$

Part I: Calculation of rated power consumption of main motor
According to (30) and (36), calculate the rolling force of each pass of rough rolling and finishing rolling;
According to (4) and (6), calculate the torque and power of the rough rolling motor and the finishing motor;
According to (39), calculate the rated power consumption of the main motor for rough rolling and finishing rolling, and obtain W;
Part II: Establishment of prediction model for additional power consumption of main motor
Create a training data set $\mathcal{D}$ for the prediction model for additional power consumption of main motor;
According to (41)–(43), the input vector of the data set $\mathcal{D}$ is dimensionally unified;
According to (44)–(50), the main motor additional power consumption prediction model is trained;
Part III: Rolling comprehensive power consumption prediction
According to (51)–(53), $\mathbf{x}$ is dimensionally expanded;
$\mathbf{x}$ is brought into the trained random forest model to obtain the additional power consumption prediction value $\hat{E}_e(\mathbf{x})$;
The rolling comprehensive power consumption $\hat{E}(\mathbf{x}) = W + \hat{E}_e(\mathbf{x})$ is given;

5. Experimental verification and result analysis

5.1. Experimental setup

The data used in this experiment comes from the medium and thick plate production line of a steel plant, which has a designed capacity of 120 t/h and operates with a single-stand four-high mill. It includes data from 12 types of steel—Q345R, S355J-2, N08811, 16MnDR, A40-T, AH36-V, D40-T, E36NH, LR-A36-V, X60MS, Q355E-3, and Q345qD-2—totalling 2,150 data points, as shown in the distribution Figure 9. The electric meter used is the Weishen DTSD341-MA2, the information transmission and exchange protocol adopts IEC 61850, and the data collection frequency is 0.01 seconds.

In the prediction stage, each data is sorted into $(\mathbf{x}_i, E_i)$, where the elements of $\mathbf{x}_i$ are given by (40), and E_i represents the comprehensive energy consumption of rolling of the steel billet. According to the calculation method in Section 3.3, the rated power consumption of the main motor W_i for each steel billet can be obtained. Let $y_i = E_i - W_i$, that is, y_i is the additional power consumption of the main motor of the billet, which gives $(\mathbf{x}_i, y_i)$, and then the data set $\mathcal{D}$. The following two experiments are used to

verify the performance of the power consumption calculation algorithm and prediction algorithm in this paper.

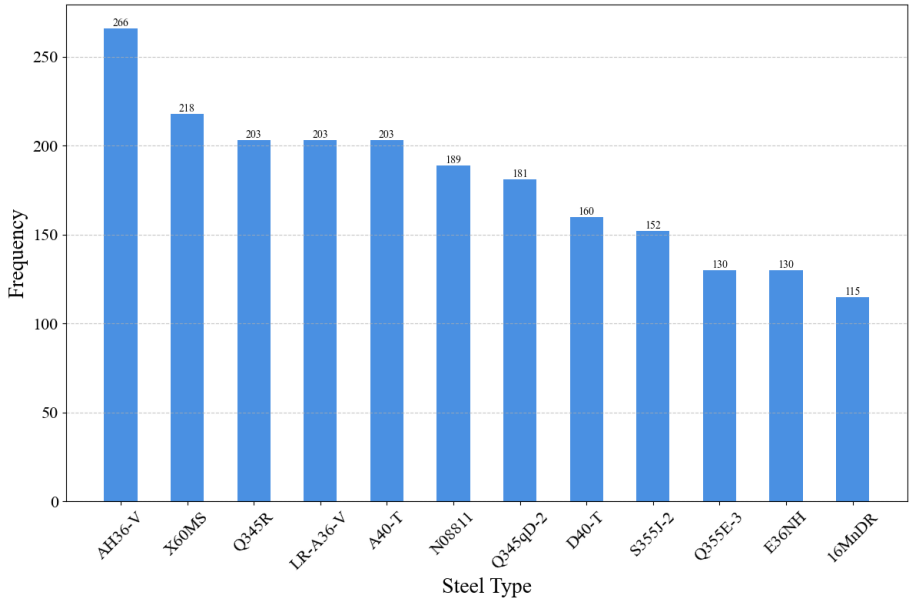


Figure 9. Steel grade distribution histogram.

Experiment 1: Performance of slab power consumption calculation algorithm

Use algorithm 1 to calculate the comprehensive rolling power consumption of each slab, and then compare it with the actual value to perform error analysis.

Experiment 2: Performance of slab power consumption prediction algorithm

Use algorithm 2 to predict the comprehensive power consumption of steel billets. In the data set, 80% of the data is used for model establishment, and the remaining 20% of the data is used for effect verification. In addition, the method in this paper is compared with the data-driven method. The data-driven method uses data in the form of $(\mathbf{x}_i, E_i)$ for model training and then make predictions.

In order to evaluate the prediction performance of the model, we select the mean absolute error (MAE, Mean Absolute Error) and the root mean square error (RMSE, Root Mean Squared Error) as the measurement criteria for model error. MAE and RMSE are commonly used regression model performance evaluation indicators, which can reflect the error between the predicted value and the actual value.

1) Mean Absolute Error (MAE):

MAE measures the average absolute difference between the predicted value and the true value, that is:

$$\text{MAE} = \frac{1}{n}\sum_{i=1}^{n}|y_i - \hat{y}_i|, \tag{54}$$

where n is the number of samples, y_i is the true value of the ith sample, and $\hat{y}_i$ is the predicted value of the ith sample. MAE can intuitively reflect the average deviation of the model prediction results by calculating the average value of the absolute error, and is insensitive to outliers. Therefore, MAE is more suitable for measuring model performance in the presence of a small number of outliers or large deviations.

2) Root Mean Square Error (RMSE):

RMSE measures the deviation between the predicted value and the true value by taking the square root of the average of the squared errors, that is:

$$\text{RMSE} = \sqrt{\frac{1}{n}\sum_{i=1}^{n}(y_i - \hat{y}_i)^2}, \tag{55}$$

Since RMSE squares larger errors, it is more sensitive to outliers. RMSE can more rigorously evaluate the predictive ability of the model, especially when the model has large errors, and can provide clearer feedback.

5.2. Results and analysis

1) Experimental results and analysis of power consumption calculation algorithm

The results of experiment 1 are shown in Figure 10, from which it can be seen that the results obtained according to algorithm 1 are approximately distributed on the $y = x$ reference line with the true value, and the MAE and RMSE of energy consumption calculation are calculated to be 7.186 and 8.161, respectively, showing that the accuracy of the calculation results of algorithm 1 is high.

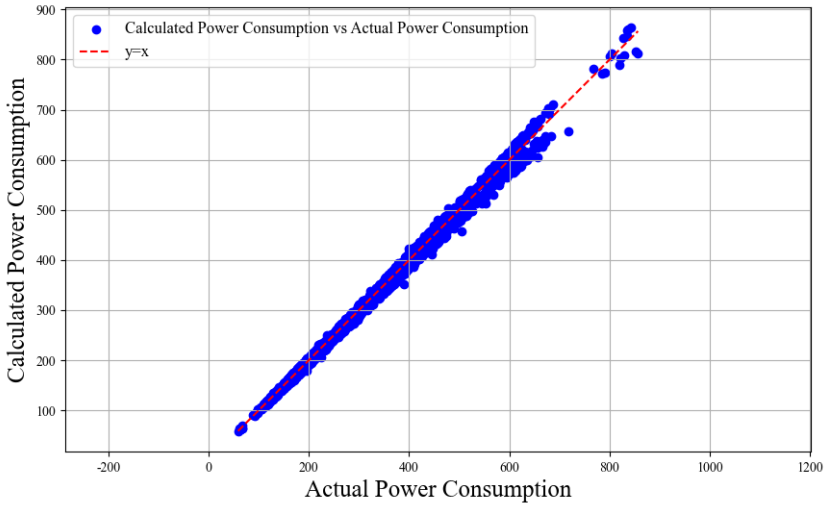


Figure 10. Comparison of the calculated value and the true value of Algorithm 1.

2) Experimental results and analysis of power consumption prediction algorithm

Table 4. Random forest parameters.

Parameter	n_estimators	max_depth	min_samples_split	min_samples_leaf	random_state
Value	3000	30	8	25	42

The parameters of random forest are shown in Table 4. The results of Experiment 2 are shown in

Figures 11–14 and Table 5. The calculated MAE and RMSE of energy consumption calculation are 10.187 and 10.962, respectively, indicating that the method in this paper has a high prediction accuracy.

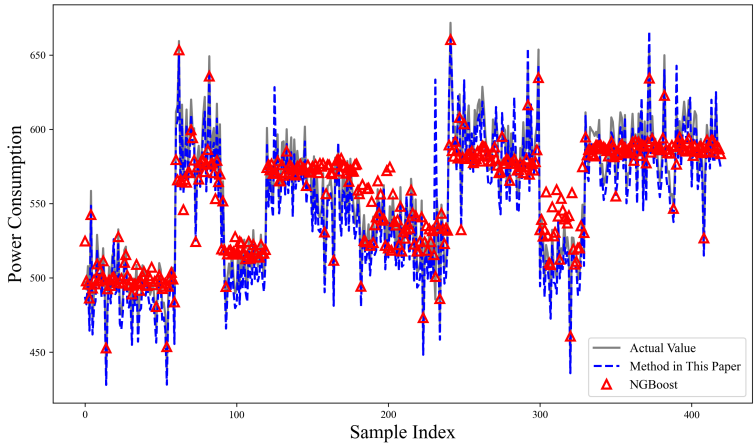


Figure 11. Method in this paper vs NGBoost.

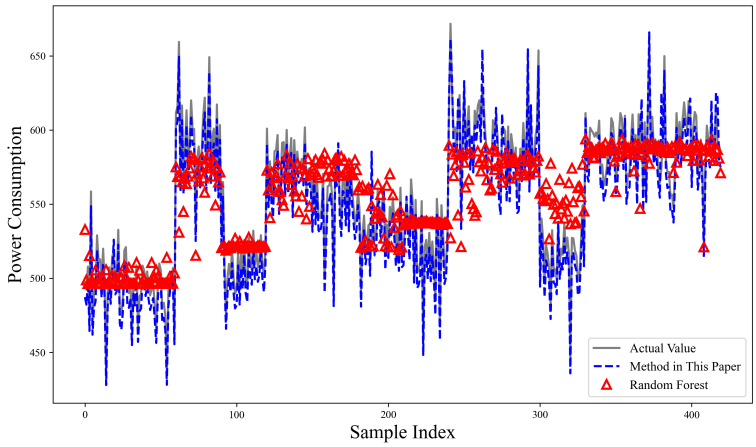


Figure 12. Method in this paper vs Random Forest.

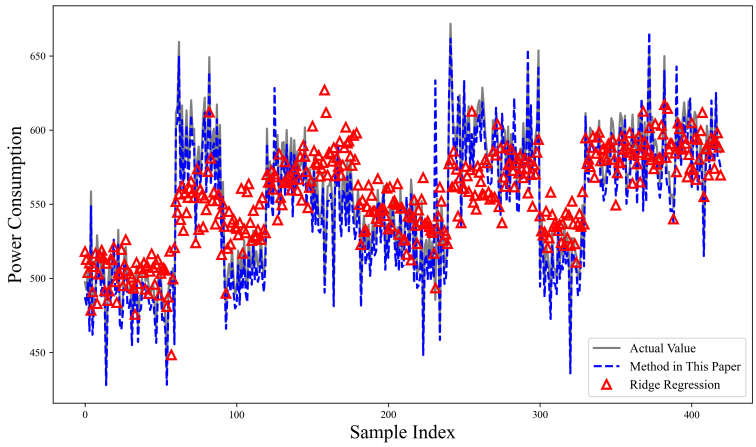


Figure 13. Method in this paper vs Ridge Regression.

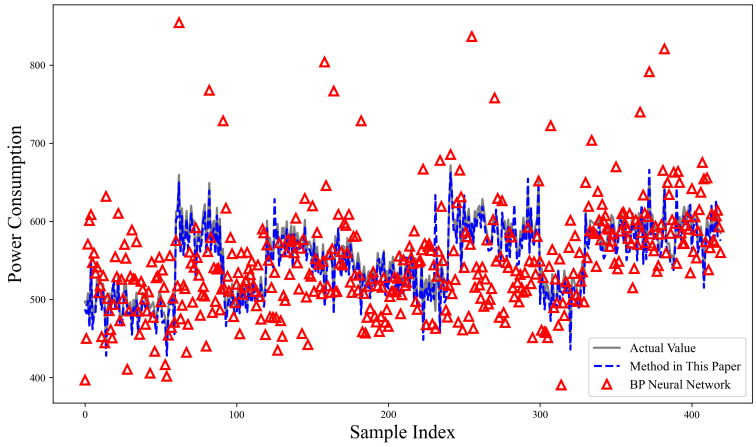


Figure 14. Method in this paper vs BP Neural Network.

Table 5. Comparison between our method and four other algorithms.

Method	MAE	RMSE
Method in this paper	10.187	10.962
NGBoost	14.190	17.681
Random Forest	21.220	28.291
Ridge Regression	24.019	31.228
BP Neural Network	50.548	67.821

6. Conclusions

In view of the problem of power consumption calculation and prediction in the rolling process of medium and thick plates, we propose a systematic solution. A time-slice based rolling power consumption calculation algorithm is introduced, employing a modular approach that divides power consumption into components for independent calculation, enhancing accuracy and adaptability; hybrid models are developed for predicting the rated power consumption of rough and finish rolling motors, combining data-driven techniques with mechanistic approaches to improve prediction accuracy; calculation methods for additional electricity consumption are proposed, utilizing the main motor power model and real-time data to estimate auxiliary system power and other components effectively.

Future power consumption prediction models are set to achieve breakthroughs in intelligence, flexibility, and accuracy through the integration of advanced technologies. By employing machine learning algorithms, big data analytics, and real-time monitoring systems, these models will refine energy consumption forecasting to a highly precise and adaptive level. Enhanced data fusion techniques will seamlessly combine historical and real-time production data, while advanced mechanistic modeling will provide deeper insights into the underlying physical processes. These models will also incorporate dynamic optimization algorithms to adjust predictions in real time, addressing process variability and uncertainties. Together, these technological advancements will elevate the accuracy and robustness of power consumption predictions in medium and thick plate rolling production.

On the other hand, we focuse on energy consumption prediction, with future research exploring how these predictions can play a role in energy optimization in rolling mills. By combining predictive models with real-time data, energy usage strategies can be dynamically adjusted during the production process, ensuring that optimal energy consumption patterns are maintained in complex production environments. This helps reduce energy waste, lower carbon emissions, and promote green manufacturing.

Use of AI tools declaration

The authors declare they have not used Artificial Intelligence (AI) tools in the creation of this article.

Conflict of interest

The authors declare there are no conflicts of interest.

References

1. Z. Han, *Research on Strategies to Enhance the Competitiveness of China's Steel Industry*, ph.D thsis, Chinese Academy of Social Sciences, 2014.
2. C. Zhang, *Research on Energy Efficiency of My Country's Steel Enterprises Based on Circular Economy*, ph.D thsis, University of Science and Technology Beijing, 2018.
3. L. Malka, F. Bidaj, A. Kuriqi, A. Jaku, R. Roçi, A. Gebremedhin, Energy system analysis with a focus on future energy demand projections: the case of Norway, *Energy*, **272** (2023), 127107. https://doi.org/10.1016/j.energy.2023.127107
4. X. Liu, S. Yuan, H. Yu, Z. Liu, How ecological policy stringency moderates the influence of industrial innovation on environmental sustainability: The role of renewable energy transition in BRICST countries, *Renewable Energy*, **207** (2023), 194–204. https://doi.org/10.1016/j.renene.2023.01.045
5. G. P. Perunov, Y. V. Inatovich, N. A. Strashkova, The power consumption optimization for thin-sheet rolling on a reversing mill, *Steel Transl.*, **50** (2020), 897–901. https://doi.org/10.3103/S0967091220120116
6. M. Tan, H. Yang, B. Duan, Y. Su, F. He, Optimizing production scheduling of steel plate hot rolling for economic load dispatch under time-of-use electricity pricing, *Math. Probl. Eng.*, **2017** (2017), 1048081. https://doi.org/10.1155/2017/1048081
7. L. Giorleo, E. Ceretti, C. Giardini, Energy consumption reduction in Ring Rolling processes: A FEM analysis, *Int. J. Mech. Sci.*, **74** (2013), 55–64. https://doi.org/10.1016/j.ijmecsci.2013.04.008
8. J. Paralikas, K. Salonitis, G. Chryssolouris, Energy efficiency of cold roll forming process, *Int. J. Adv. Manuf. Technol.*, **66** (2013), 1271–1284. https://doi.org/10.1007/s00170-012-4405-8
9. V. Chubenko, A. Khinotskaya, T. Yarosh, L. Saithareiev, Sustainable development of the steel plate hot rolling technology due to energy-power process parameters justification, in *E3S Web of Conferences*, EDP Sciences, **166** (2020), 06009.

10. J. Qiu, J. Feng, X. Huang, Z. Huang, Optimization of reheating furnace rolling delay strategies based on a minimum energy consumption principle, *J. Iron. Steel Res. Int.*, **2024** (2024), 1–13. https://doi.org/10.1007/s42243-024-01227-0
11. X. Chen, Y. Yang, Data-driven multi-objective optimization of power consumption and quality for finishing rolling process, in *2024 IEEE 13th Data Driven Control and Learning Systems Conference (DDCLS)*, IEEE, (2024), 1262–1266. https://doi.org/10.1109/DDCLS61622.2024.10606881
12. Y. Zhong, J. Wang, J. Xu, S. Wu, J. Rao, K. Dang, Prediction of energy consumption in horizontal roughing process of hot rolling strip based on TDADE algorithm, *IEEE Trans. Autom. Sci. Eng.*, **21** (2023), 555–568. https://doi.org/10.1109/TASE.2023.3236306
13. Y. T. Kim, B. J. Kim, S. W. Kim, Multi-level stacked regression for predicting electricity consumption of hot rolling mill, *Expert Syst. Appl.*, **201** (2022), 117040. https://doi.org/10.1016/j.eswa.2022.117040
14. X. Xiong, D. Deng, Y. Xiao, Q. Guo, Y. Zhang, Research on prediction method of finish rolling power consumption of multi-specific strip steel based on random forest optimization model, in *2020 39th Chinese Control Conference (CCC)*, IEEE, (2020), 5977–5984. https://doi.org/10.23919/CCC50068.2020.9188937
15. S. Behzadipour, A. Khajepour, J. G. Lenard, J. Biglou, A new shape change quantification method for estimation of power in shape rolling, *J. Mater. Process. Technol.*, **148** (2004), 353–361. https://doi.org/10.1016/j.jmatprotec.2004.02.047
16. G. A. Orcajo, J. Rodríguez, P. Ardura, J. M. Cano, J. G. Norniella, T. R. Llera, et al., Dynamic estimation of electrical demand in hot rolling mills, *IEEE Trans. Ind. Appl.*, **52** (2016), 2714–2723. https://doi.org/10.1109/TIA.2016.2533483
17. Y. Sun, *Model and Control of Hot Strip Rolling*, Metallurgical Industry Press, Beijing, 2007.
18. R. B. Sims, The calculation of roll force and torque in hot rolling, *Proc. Inst. Mech. Eng.*, **168** (1954), 191–200. https://doi.org/10.1243/PIME_PROC_1954_168_023_02
19. J. Guo, X. Wang, W. Xue, Y. Zhao, System identification with binary-valued observations under data tampering attacks, *IEEE Trans. Autom. Control*, **66** (2021), 3825–3832. https://doi.org/10.1109/TAC.2020.3029325
20. J. Guo, Q. Zhang, Y. Zhao, Identification of FIR Systems with binary-valued observations under replay attacks, *Automatica*, **172** (2025), 112001. https://doi.org/10.1016/j.automatica.2024.112001

21. H. Valecha, A. Varma, I. Khare, A. Sachdeva, M. Goyal, Prediction of consumer behaviour using random forest algorithm, in *2018 5th IEEE Uttar Pradesh Section International Conference on Electrical, Electronics and Computer Engineering (UPCON)*, IEEE, (2018), 1–6. https://doi.org/10.1109/UPCON.2018.8597070



AIMS Press

© 2025 the Author(s), licensee AIMS Press. This is an open access article distributed under the terms of the Creative Commons Attribution License (http://creativecommons.org/licenses/by/4.0)